NASA TECHNICAL TRANSLATION NASA TT F-15,955

ENERGY FLOW IN ELECTROMAGNETIC WAVE FIELDS

H. Landstorfer, H. Liska, H. Meinke and B. Müller

(NASA-TT-F-15955) ENERGY FLOW IN ELECTROMAGNETIC WAVE FIELDS (Kanner (Leo) Associates) 20 p HC $4.00 CSCL 20N

N74-34596

Unclas
G3/07 50372

Translation of "Energieströmung in elektromagnetischen Wellenfeldern," Nachrichtentechnische Zeitschrift (NTZ-Communications Journal), Vol. 25, No. 5, 1972, pp. 225-231

NATIONAL AERONAUTICS AND SPACE ADMINISTRATION
WASHINGTON, D.C. 20546 OCTOBER 1974

ENERGY FLOW IN ELECTROMAGNETIC WAVE FIELDS

H. Landstorfer, H. Liska, H. Meinke and B. Müller

Preliminary Remark

/225*

In his field equations, Maxwell chose to represent field behavior by means of field strengths. This undoubtedly was due to historical reasons. We are of the view that field strengths provide more of a formal mathematical description of the state of the field, whereas the distribution, motion and conversion of energy (conversion of electrical energy into magnetic energy and vice versa) represent the actual physical process. It appears possible that better information concerning the behavior of energy may also result in an improved understanding of electromagnetic processes. A better physical understanding would assist the engineer in all of those complex cases in which mathematical computation is not feasible or is no longer reasonable because of the high mathematical outlay. Unfortunately, a great many practical applications involving electromagnetic waves belong among the noncalculable cases, due to the severe boundary conditions and have only been amenable to experimental research so far.

1. Instantaneous Energy Flow

The Poynting vector, called the vector of energy flow density in the following [5a], indicates the direction of energy flow, via its own direction, and energy transport per unit time, referred to the unit of area, via its length. In time-variable fields, it is defined for the time being as the time-variable vector **s** of instantaneous energy flow density

---

* Numbers in the margin indicate pagination in the foreign text.

$$\mathbf{s} = \mathbf{e} \times \mathbf{h} \tag{1}$$

As shown in Fig. 1, it is perpendicular to the vector e of instantaneous electric field strength and to the vector h of instantaneous magnetic field strength. Its length is

$$|s| = |e| \cdot |h| \cdot \cos \alpha \tag{2}$$

where α is the angle between the spatial vectors **e** and **h**. Our studies on instantaneous energy movement [4] have shown that very complex and difficultly understood energy behavior occurs even in relatively simple cases. Moreover, all time-variable field processes have the basic disadvantage that they can be represented only through a series of pictures, e.g. instantaneous patterns; the result actually becomes completely recognizable only as a motion picture. The presentation of such a sequence of pictures in a book or journal is expensive and yet not very satisfactory. The reader is referred to our instantaneous patterns of the near field of an antenna in [1] and [2], which are considerably clearer in effect in a motion picture which has been made.

2. Time-Averaged Energy Flow

Plotting the vector of time-averaged energy flow density, which thus indicates the mean of energy transport over time at a given location in terms of direction and magnitude, has proven to be particularly simple and informative. This method was introduced by Wolter [3]. At each point in the field, there is thus a vector, constant over time, which indicates the direction of mean energy flow and its mean magnitude at this point. Actual energy movement is the result of superimposing an oscillation over this mean movement; cf. Section 3. We can then show streamlines for time-averaged energy flow in this space on the basis of known principles of flow theory; the vectors of time-averaged energy flow density are tangents to the streamlines. Such a

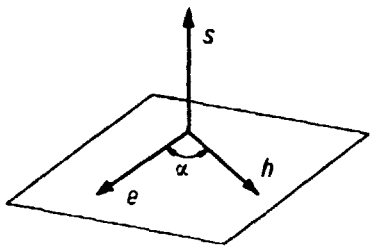

Fig. 1. Vector of energy flow density (Poynting vector).

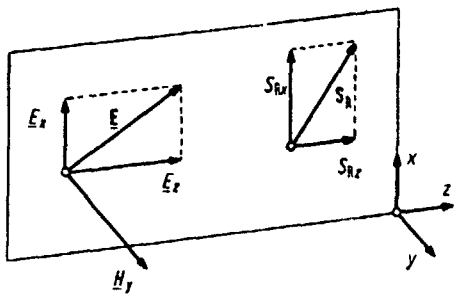

Fig. 2. Vectors of a TM wave.

streamline pattern is very similar to stationary flow in a source-free fluid.

We obtain time-averaged energy transport by means of a generalized pattern of effective values with the aid of complex amplitudes. In a rectangular coordinate system (Fig. 2), complex electric field strength vector $\underline{\mathbf{E}}$ has the complex components

$$\underline{E}_x = E_x \cdot e^{j\varphi_x}; \quad \underline{E}_y = E_y \cdot e^{j\varphi_y}; \quad \underline{E}_z = E_z \cdot e^{j\varphi_z}. \quad (3)$$

Complex magnetic field strength vector $\underline{\mathbf{H}}$ has the complex components

$$\underline{H}_x = H_x \cdot e^{j\varphi_x}; \quad \underline{H}_y = H_y \cdot e^{j\varphi_y}; \quad \underline{H}_z = H_z \cdot e^{j\varphi_z}. \quad (4)$$

As an expansion of equation (1), we can define a complex vector for energy flow density [6]

$$\underline{S} = S_R + j S_I = \frac{1}{2}(\underline{E} \times \underline{H}^*). \quad (5)$$

$\underline{\mathbf{H}}^*$ is the complex conjugate vector of magnetic field strength. /226
This definition of energy flow density is a generalization of the formula for complex apparent power, in which one of the two coefficients also appears with its complex conjugate value. The coefficient 1/2 always occurs in effective values when field strengths are given in peak values.

The transport of real power is described by the real part, S_R. S_R is the actual energy flow density, which also establishes

the direction of streamlines. The direction of S_R is the mean propagation direction of the energy. The imaginary part S_I from equation (5) represents a reactive power density and describes an oscillating movement of energy about its time-averaged movement (see Section 3).

The formula for real part S_R is relatively extensive for general three-dimensional wave processes, so two simpler examples will merely be considered formally in the following. Fig. 2 shows the first case. Here, the electric fields of the wave lie in an x-z plane, and magnetic field $\underline{H}_y$ is perpendicular to the plane (TM wave). Fig. 3 shows the second case, in which magnetic field lies in a plane with components $\underline{H}_x$ and $\underline{H}_z$, and electric field is perpendicular to this plane as an $\underline{E}_y$ component (TE wave). From the convention in Fig. 1, with $\alpha = 90°$, components $\underline{E}_x$ and $\underline{H}_y$ from equations (3) and (4) form the component S_{Rz} of time-averaged energy flow density in Fig. 2:

$$S_{Rz} = \frac{1}{2} E_x H_y \cdot \cos(\psi_x - \varphi_y) \tag{6}$$

and components $\underline{E}_z$ and $\underline{H}_y$ form the component S_{Rx} of energy flow:

$$S_{Rx} = -\frac{1}{2} E_z H_y \cdot \cos(\psi_z - \varphi_y). \tag{7}$$

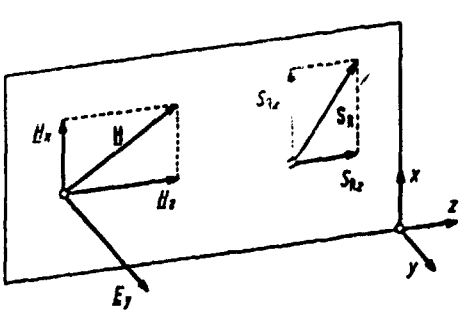

Fig. 3. Vectors of a TE wave.

The (mathematically) positive directions of the components of field strength and energy flow density are diagrammed in Fig. 2. If we apply the convention in Fig. 1 to component S_{Rx}, then, according to equation (7), S_{Rx} must be shown in the negative direction.

In Fig. 3, components $\underline{E}_y$ and $\underline{H}_x$ form the component S_{Rz} of energy flow:

$$S_{Rz} = -\frac{1}{2} E_y H_x \cdot \cos(\psi_y - \varphi_x) \cdot \tag{8}$$

likewise, components $\underline{E}_y$ and $\underline{H}_z$ form the component S_{Rx} of energy flow:

$$S_{Rx} = \frac{1}{2} E_y H_z \cdot \cos(\psi_y - \varphi_z) . \tag{9}$$

In these two special cases, the energy streamlines lie in the plane given and thus can be represented graphically by simple means. With the exception of a three-dimensional case in Fig. 13, only planar cases will be represented in the following. As is conventional for planar flows, the streamlines are drawn at distances such that equal energy flows move between each pair of adjacent streamlines. Thus the distance between streamlines in such pictures is a measure of flow density. A small interval indicates high flow density.

3. Ellipse of the Instantaneous Vector of Energy Flow

It is shown in [7] that in the special cases shown in Figs. 2 and 3, instantaneous vector $\mathfrak{s}(t)$ in equation (1) is obtained from the time-averaged value S_R in equations (6) through (9) with an additional time-dependent vector $\Delta\mathfrak{s}(t)$:

$$\mathfrak{s}(t) = S_R + \Delta\mathfrak{s}(t). \tag{10}$$

This $\Delta\mathfrak{s}$ follows an ellipse with time, as shown in Fig. 4, in such a manner that $\mathfrak{s}$ becomes zero at a certain time. S_R and S_I are conjugate diameters of the ellipse, and the ellipse can be constructed from these two vectors by known methods. In a

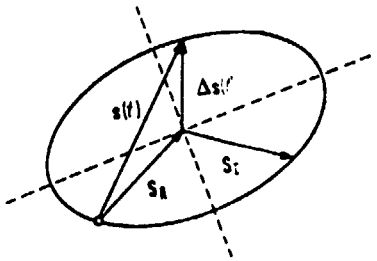

Fig. 4. Ellipse of the complex vector of energy flow density.

plane wave with linear propagation,

$$s(t) = S_R[1 + \cos(\omega t + \delta)], \qquad (11)$$

and the ellipse degenerates into a straight line which has the direction of S_R. The ellipse thus describes the periodic oscillations superimposed on time-averaged energy flow. In a certain way, the transverse oscillations represent a reactive power in the field. We suspect that this reactive power has an effect on the behaviors of streamlines for real power.

4. Energy Velocity

If we wish to characterize the movement of energy in a wave field in detail, we must define an energy velocity. In a plane TEM wave, linear movement occurs everywhere and at all times and is at the velocity of light. In a more general wave field, energy /227 velocity, in terms of direction and magnitude, is a function of position and time. This applies to waves in homogeneous waveguides.

The energy dW in an infinitesimal volume element dV will be called an energy packet. The energy packet moves at the instantaneous energy velocity associated with the particular location and time. A definition of velocity is not without problems, in that the identity of the energy packet as an individual cannot be determined along its path by measurement. A definition of velocity for unidentifiable individual entities is always of a purely formal nature, but must be free of contradiction, i.e. must be compatible with all measured physical phenomena. In spite of this difficulty, we believe that the energy velocity defined by us can provide certain presentational advantages and

makes certain verifiable conclusions possible, and thus is certainly more than a pure formalism.

A noncontradictory definition for a velocity vector is obtained if, in analogy to fluids, we define velocity as the quotient of energy flow density and energy density [4]. If we use instantaneous values $\mathbf{s}$ for flow density and w for energy density here, we obtain the vector $\mathbf{v}$ of instantaneous energy velocity

$$\mathbf{v} = \mathbf{s}/w. \tag{12}$$

If we use the time-averaged values S_R for flow density and w_m for energy density, we obtain mean energy velocity

$$\mathbf{v}_m = S_R/w_m. \tag{13}$$

With the aid of instantaneous velocity $\mathbf{v}$, we can calculate the path covered by an energy packet with time (instantaneous path; cf. Figs. 6, 7 and 9). With the aid of mean velocity, we obtain the mean path of the energy packet along the mean streamline, since vector $\mathbf{v}_m$ always has the direction of S_R.

5. Homogeneous and Inhomogeneous Waves between Conducting Planes

Fig. 5 shows a plane TEM wave between conducting planes. The case is that shown in Fig. 2, with $E_z = 0$. Only E_x exists. The electric flux lines are parallel vertical lines in direction E. Since the magnetic flux lines are perpendicular to the plane of the drawing, as in Fig. 2, energy flow has only a z-component. The horizontal lines marked with arrows are the instantaneous and time-averaged streamlines. The streamlines have the same interval between one another, and mean flow density is the same across the entire waveguide cross section.

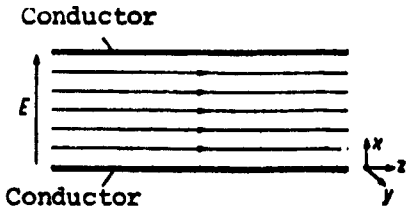

Fig. 5. Energy streamlines in a TEM wave.

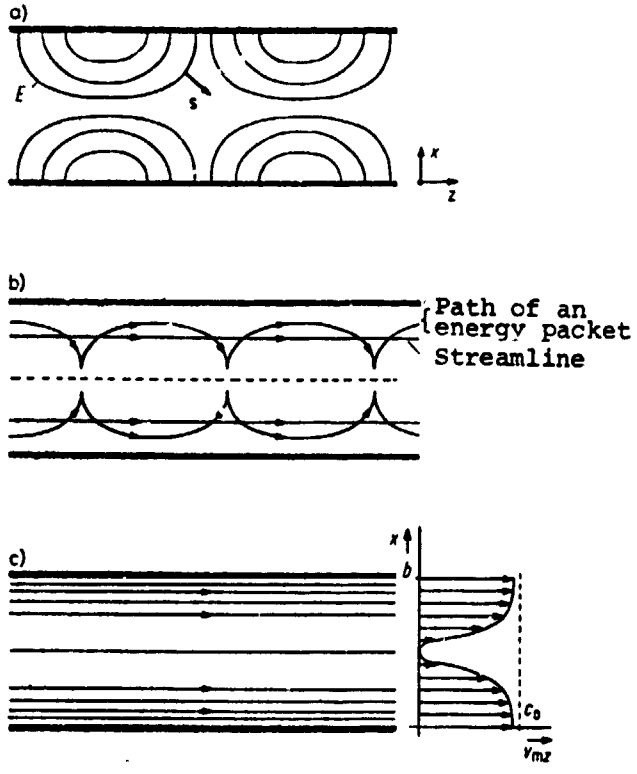

Fig. 6. TM wave between parallel conducting plane. a) Instantaneous electric flux lines, b) Instantaneous and time-averaged paths of an energy packet, c) Mean energy flow and mean energy velocity.

Fig. 6a shows the instantaneous electric flux lines of a TM wave between parallel conducting planes [8]. This is a case of the type shown in Fig. 2 with time-dependent e_x and e_z. /228 From Fig. 1, with $\alpha = 90°$, instantaneous energy flow **s** is perpendicular to the instantaneous electric lines of flux. Since the lines of flux move, magnitude and direction of energy flow density are continually changing. Instantaneous velocity has components in the x-direction and z-direction. As an example, Fig. 6b shows a characteristic path of an energy packet which makes not only a longitudinal movement but also tranverse oscillations. Energy movement is symmetrical with respect to the dashed center line, along which $S_R = 0$ at all times and across which no energy therefore travels. Time-averaged energy flow has only a z-component, and the streamlines are straight lines in the z-direction. The distribution of time-averaged energy flow over the cross section is not uniform, as the distance between adjacent energy streamlines shows in Fig. 6c.

A concentration of energy flow density occurs close to the bounding conducting planes. Time-averaged energy velocity is a function of x. Fig. 6c shows the distribution of energy velocity v_{mz}, defined by equation (13), over the cross section on the right.

Fig. 7 shows the instantaneous magnetic flux lines of a TE wave between parallel conducting planes. This is a case like that shown in Fig. 3, with time-variable h_x and h_z:

$$e_y = E_y(x) \cdot \cos(\omega t - \beta z); \tag{14}$$

$$h_x = H_x(x) \cdot \cos(\omega t - \beta z); \tag{15}$$

$$h_z = H_z(x) \cdot \sin(\omega t - \beta z). \tag{16}$$

Instantaneous energy flow **s** is perpendicular to the instantaneous magnetic flux lines. It has the components

$$s_z = e_y h_z = \frac{1}{2} E_y H_z \cdot \sin 2(\omega t - \beta z); \tag{17}$$

$$s_x = -e_y h_x = -\frac{1}{2} E_y H_x [1 + \cos 2(\omega t - \beta z)]; \tag{18}$$

s_x varies at twice the frequency but vanishes in the average over time. The component of instantaneous energy flow s_z contains not only the alternating part $\cos 2(\omega t - \beta z)$ but also a part independent of time, identical to the time average of energy flow S_{Rz}. Energy density w can likewise be resolved into a DC part and an AC part, the DC part being identical to mean energy w_m:

$$w = \frac{1}{4}(\varepsilon_0 E_y^2 + \mu_0 H_x^2 + \mu_0 H_z^2) + \\ + \frac{1}{4}(\varepsilon_0 E_y^2 + \mu_0 H_x^2 - \mu_0 H_z^2) \cdot \cos 2(\omega t - \beta z). \tag{19}$$

Instantaneous velocity has components v_x in the x-direction (transverse oscillation) and v_z in the z-direction (longitudinal

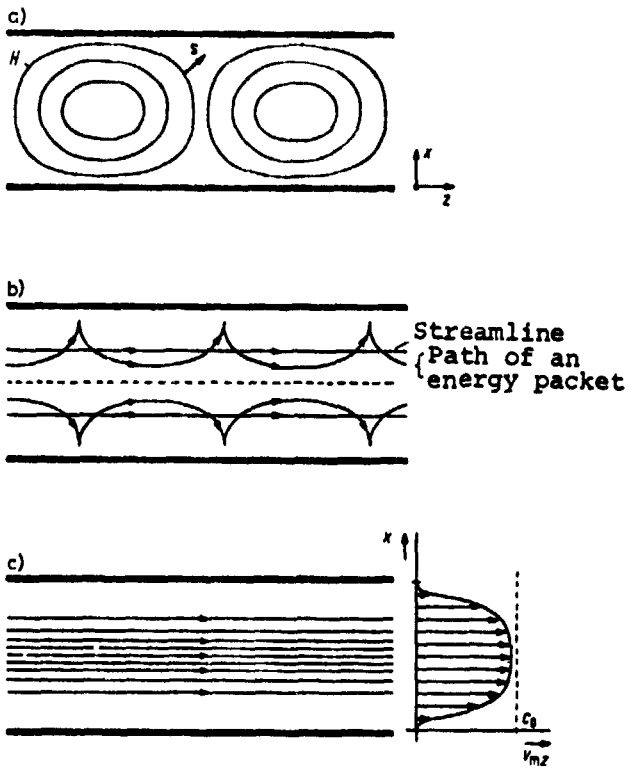

Fig. 7. TE wave between parallel conducting planes. a) Instantaneous magnetic flux lines, b) Instantaneous and time-averaged paths of an energy packet; c) Mean energy flow and mean energy velocity.

movement). As an example, Fig. 7b shows the characteristic path of an energy packet with transverse oscillation. Energy movement is symmetrical with respect to the dashed center line, on which $S_{Rx} = 0$, i.e. only S_{Rz} exists. Time-averaged energy flow has only a z-component. The streamlines are straight lines in the z-direction. Time averaged energy flow is distributed nonuniformly over the cross section, as the distance between adjacent streamlines in Fig. 7c shows. A concentration of energy flow density occurs at the center of the waveguide. Fig. 7c shows the distribution of mean energy velocity v_{mz} over the cross section on the right. The nonuniform distribution of energy velocity explains the familiar problems involved in transmitting modulated signals with waveguides. Signals appear at the output of the waveguide with distorted modulation because they move faster at the inside, on the average, than at the outside. This effect is also referred to as the dispersion of a waveguide.

Fig. 8 shows the ellipses of instantaneous flow density for a cross-sectional plane of the waveguide as an example for Fig. 4. Along the center line, the ellipse degenerates into a straight line, since $S_{Rx} = 0$.

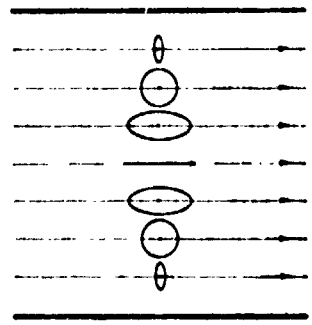

Fig. 8. Ellipses of the complex vector of energy flow density (Fig. 4) in a TE wave between parallel conducting planes (Fig. 7).

Fig. 9 shows the mean streamlines in an elbow and, in the form of a dashed line, an example of the instantaneous path of an energy packet [4]. In the curved region, energy is "pushed" outward somewhat, on the average (by a sort of centrifugal force), and the instantaneous movement exhibits certain transverse oscillations there.

Fig. 10a shows mean streamlines where a waveguide of parallel conducting planes widens abruptly, at a relatively low frequency, at which the higher modes are still quite aperiodic in inhomogeneity. Excitation is produced by a TEM wave arriving from the t. E is the direct f electric flux l in the homogeneous region. The energy flow behaves almost as in the potential flow of an incompressible fluid.

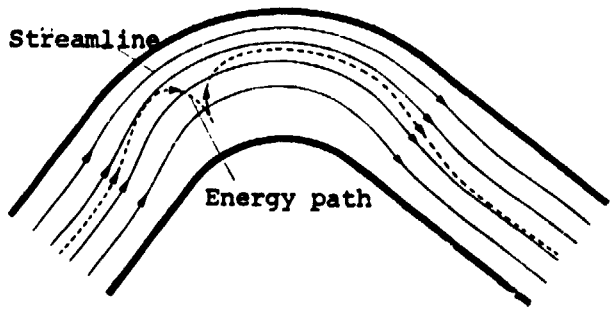

Fig. 9. Streamlines in a curved waveguide. Example of an instantaneous energy path.

Fig. 10b shows the mean streamlines at a higher frequency, at which a low-energy region develops at the lower wall. The upper corner apparently has a suction effect at higher frequencies, so energy flows upward there. The resultant low-energy region on /229 the lower conductor draws the energy downward again, and thus transverse oscillations arise in the energy flow, not only transverse oscillations in instantaneous energy flow, as in Fig. 9, but also transverse oscillations in time-averaged energy flow.

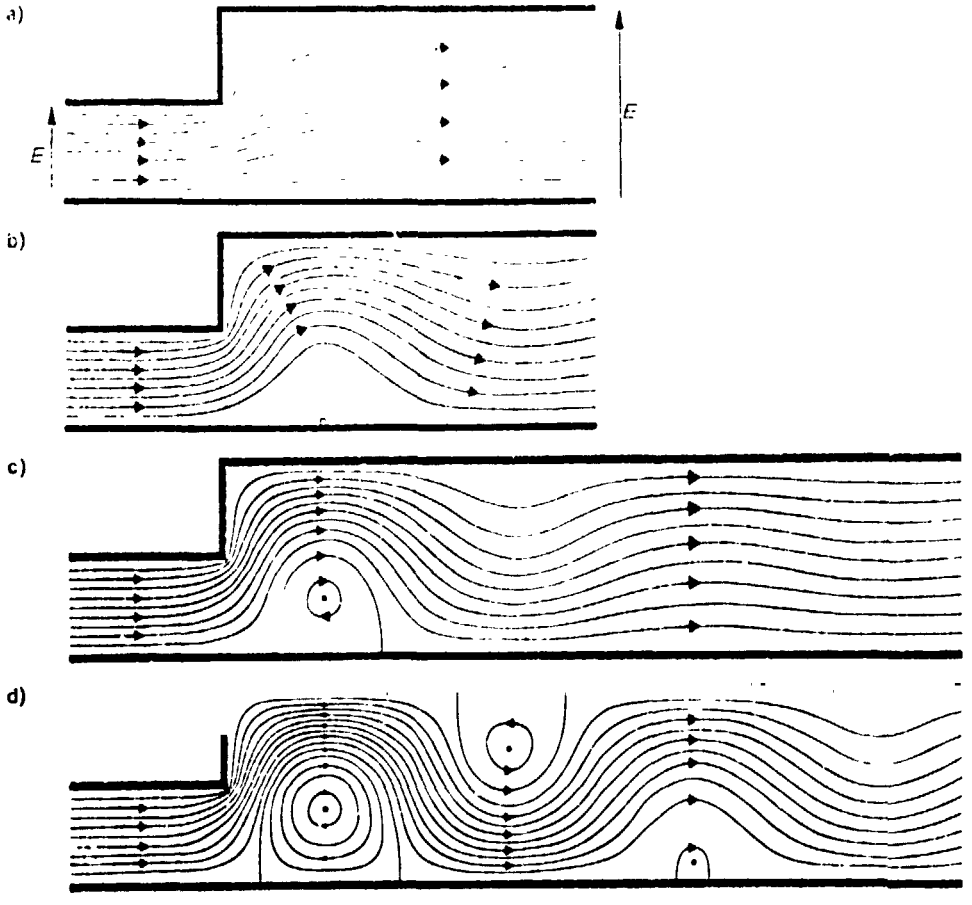

Fig. 10 Mean energy streamlines in a strip line which abruptly widens to width b. a) At a relatively low frequency ($2b/\lambda = 0.5$), b) with a low-energy region ($2b/\lambda_0 = 0.93$), c) with an energy vortex ($2b/\lambda = 0.96$), d) with a multiple vortex ($2b/\lambda = 0.99$).

Fig. 10c shows an even higher frequency at which an energy vortex has developed [9]. Such vortices accompany very pronounced transverse oscillations in energy. These transverse oscillations can produce a series of sequential vortices.

Fig. 10d shows energy streamlines in a multiple vortex. The vortices fill out each of the spaces which are freed of advancing energy by the transverse oscillations. A constant quantity of energy rotates in the vortex region, when averaged over time.

In such complex wave fields, the instantaneous movements are already becoming so difficult to follows [4] that they no longer provide any information. The mean streamlines, on the other hand, provide information on the behavior of inhomogeneity. For example, the vortex in Fig. 10c blocks the passage of energy in the region of the vortex, thereby reducing the effective cross section of the waveguide and lengthening the path of transported energy. The vortex can easily be detected with instruments through its effect on the inhomogeneity reflection factor; see also [9].

6. Near Field of Rod Antennas

Fig. 11 shows energy flow for a short rod antenna which is standing on a conducting plane and is fed coaxially. The cylindrically symmetrical fields have the character shown in Fig. 2. The fields were calculated in [7] and [10]. While conventional theories assume unrealistic slot feed, realistic feed through a coaxial line of finite size is treated here for the first time in an exact theory. Only in this way does it become possible to show how energy leaves the coaxial line into space along the streamlines. Fig. 11a shows the distribution of time-average vector S_R of energy flow density, and Fig. 11b shows the associated streamlines [12]. It can be seen here that the rod antenna does not "radiate"; rather, the energy moving from bottom to top in the coaxial feed line is altered in its direction of movement by the energy distribution that builds up in the antenna's near field and is distributed within the surrounding space. This change in streamline direction results from transverse energy oscillations, visible only in the instantaneous movement of energy, but still not in the mean streamlines in the case of short rods. These instantaneous transverse oscillations, which represent a type of reactive power in the field, can be seen from the imaginary part S_I of energy flow density from equation (5) and the ellipses of complex energy flow density.

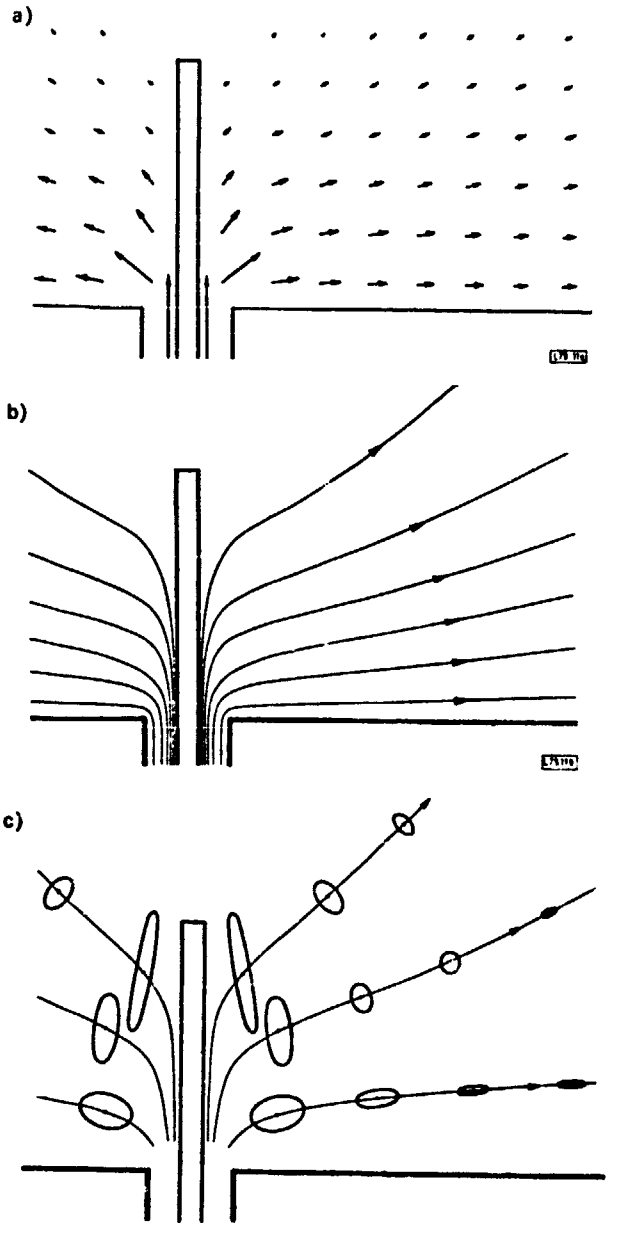

Fig. 11. Mean energy flow of a short rod antenna of length $\lambda/10$. a) Distribution of the vector S_R of time-averaged energy flow density; b) Energy streamlines associated with Fig. 11a; c) Ellipses of the complex energy flow density vector along three energy streamlines from Fig. 11b.

As an example, Fig. 11c shows these ellipses along three streamlines from Fig. 11b. The dimensions of the ellipses perpendicular to the streamlines are a good measure of the magnitude of transverse oscillations. The ellipses become flatter and the oscillations smaller with increasing distance from the antenna.

If the rod is made longer, the transverse oscillations become larger and also visible on the mean streamlines. Fig. 12 shows the streamlines in the region around a longer rod. Once the mean streamlines oscillate visibly back and forth, as in Fig. 12, the far field pattern /230 moves away from the familiar vertical pattern of the short radiator. Pronounced transverse oscillations produce a lobing of the far field pattern. In the future it should be possible to explain the behavior of a wave in the far field quantitatively,

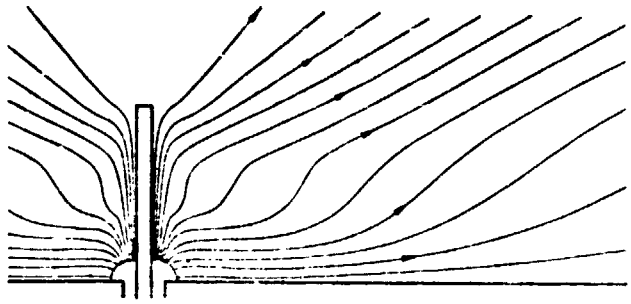

Fig. 12. Mean energy streamlines of a rod antenna of length λ.

too, on the basis of transverse energy oscillations in the antenna's near field.

7. Effective Area of Receiving Antennas

The near field of receiving antennas has been calculated in [11]. Representing the field with flux lines proves to be problematical and unclear here, since the flux lines require a time-variable three-dimensional mode of representation (superposition of a plane and a cylindrically symmetrical wave field). On the other hand, it is again simple and informative to describe the reception process with streamlines of time-averaged energy flow in this case [13].

Fig. 13 shows a short rod antenna above a conducting plane, acting as a receiving antenna. A complex resistance Z equal to /231 the complex conjugate impedance of the rod (internal resistance of source) exists between the base of the rod antenna and the conducting plane, acting as the dissipator of received power. It is that dissipator which draws the maximum possible (available) real power from the receiving antenna. A plane TEM wave passes along the conducting plane, from right to left in Fig. 13, with electric field perpendicular to the conducting plane. Fig. 13a shows the distribution of the vector of time-averaged energy flow density in a vertical plane through the radiator. From these vectors we obtain the streamlines shown in the vertical plane in Fig. 13b. Fig. 13b also shows the streamlines in the horizontal conducting plane in perspective. The linear intersection of the two planes shown is the direction of the arriving wave. There are boundary streamlines which divide the wave field into two regions. Two such boundaries are shown with dashed lines

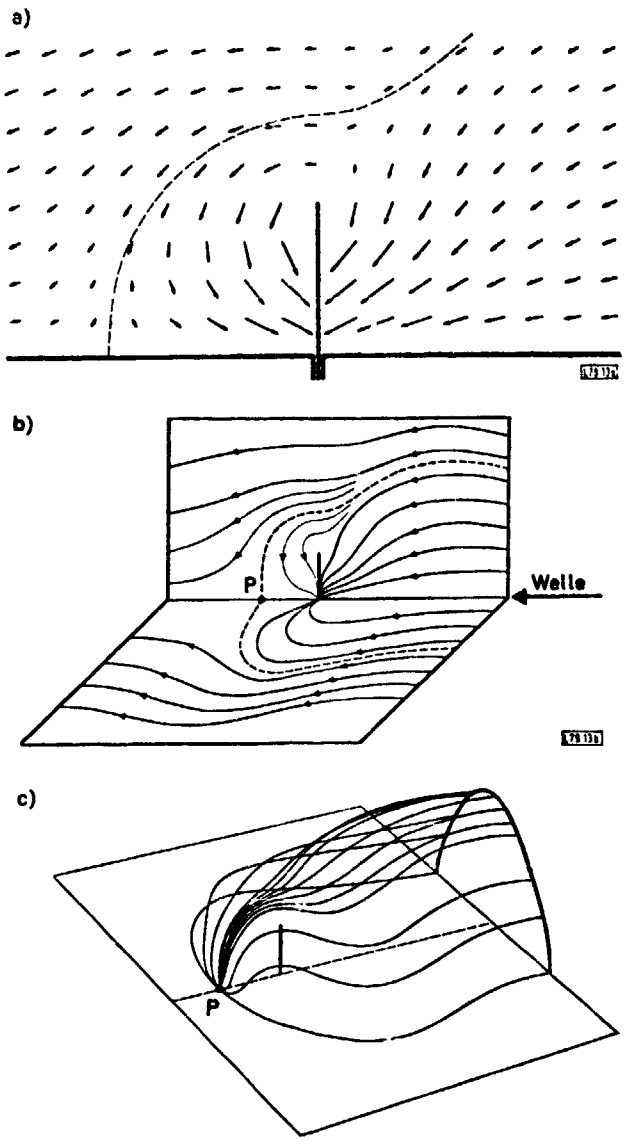

Fig. 13. Mean energy flow of a short receiving antenna. a) Distribution of the vector S_R of time-averaged energy flow density in a vertical plane through the radiator. The boundary streamline is dashed in. b) Mean energy streamlines (the horizontal plane is shown in perspective). c) Perspective representation of boundary streamlines.

In the vertical plane in Fig. 13b, all those streamlines move into the base of the antenna which are located under the boundary. All streamlines above the boundary go past the antenna. The boundary thus separates that part of the wave which passes into the receiving antenna. Likewise Fig. 13b shows the dashed boundary in the horizontal plane. All of the boundary streamlines are shown together in perspective in Fig. 13c. They terminate at point P, perpendicular to the line which passes through the base of the antenna and is in the direction of the arriving wave, and they delimit a certain space. All streamlines outside this space flow past the receiving antenna. The streamlines within the delimited area all terminate at the base

of the receiving antenna in dissipator Z. The energy transported along these streamlines yields the received power. The boundary streamlines asymptotically approach straight lines parallel to the direction of the wave with increasing distance from the receiving antenna. The area delimited by them asymptotically approachs a cross section in the process which represents the effective area of the antenna, for the energy of the arriving plane wave passing through this area is absorbed by a receiving antenna with optimum dissipator Z, and this is the definition of effective area. We obtain information regarding the shape of this effective area for the first time in this manner. The size of the effective area produced in this manner is equal to the values obtained theoretically, to several percent, within the range of feasible numerical precision, e.g. $3\lambda^2/16\pi$ for short rods. Effective area has been calculated for various rod lengths. The height of the effective area increases with increasing rod height and is greater than rod height. Its width decreases with increasing rod height [13].

The possibility of calculating the shape of the effective area is an interesting indication of the extensive new information about complex electromagnetic wave fields which can be obtained by calculating energy streamlines. The system of streamlines can be supplemented with a family of orthogonal curves, which we call "phase lines." These phase lines describe the time taken by the wave process along the streamlines.

REFERENCES

1. Liska, H., Meinke, H., and Mohr, C., "Wave separation from a conical antenna," Nachrichtentech. Z. 23, 74-79 (1970).

2. Landstorfer, F., "Wave separation from rod antennas," Nachrichtentech. Z. 23, 273-278 (1970).

3. Wolter, H., "The problem of the path of light in total reflection," Z. Naturforsch. 5A, 276-283 (1950).

4. Liska, H., "Energy transport in electromagnetic wave fields," dissertation, Munich Engineering University, 1970.

5. Macke, W., Elektromagnetische Felder [Electromagnetic Fields], Section 134, "The streamline pattern," 3rd edition, Leipzig, 1965.

5a. Ibid., Section 614.

6. Meinke, H.H. and Gundlach, F.W., Taschenbuch der Hochfrequenztechnik [Handbook of Radio Frequency Engineering], Section H4, 3rd edition, Berlin, Springer-Verlag, 1968.

7. Landstorfer, F., "Wave separation and energy transport in the near fields of rod antennas used for transmission," habilitation paper, Munich Engineering University, 1971.

8. Meinke, H., Einführung in die Elektrotechnik höherer Frequenzen [Introduction to Radio Frequency Electrical Engineering], Section II.1, Vol. 2, 2nd edition, Berlin, Springer-Verlag, 1966.

9. Liska, H., " Experimental evidence of the two elementary types of energy vortices in wave fields," Nachrichtentech. Z. 23, 445-448 (1970).

10. Landstorfer, F., "Admittance and current distribution cf linear cylindrical rod antennas," Arch. elektr. Übertr. 23, 61-69 (1969).

11. Müller, B., "Calculating the electromagnetic field about a receiving antenna," Arch. Elektron. Übertr.-techn. 26 (1972) (in press).

12. Landstorfer, F., "Energy transport in the near field of rod antennas," Arch. Elektron. Übertr.-techn. 26 (1972) (in press).

13. Müller, B., "Calculating energy flow in the near field of a receiving antenna," Arch. Elektron. Übertr.-techn. 26 (1972) (in press).